CapST: An Enhanced and Lightweight Model Attribution Approach for Synthetic Videos

Wasim Ahmad, Yan-Tsung Peng *Member, IEEE*, , Yuan-Hao Chang *Fellow, IEEE*, , Gaddisa Olani Ganfure, Sarwar Khan, Sahibzada Adil Shahzad

Abstract—Deepfake videos, generated through AI faceswapping techniques, have garnered considerable attention due to their potential for powerful impersonation attacks. While existing research primarily focuses on binary classification to discern between real and fake videos, however determining the specific generation model for a fake video is crucial for forensic investigation. Addressing this gap, this paper investigates the model attribution problem of Deepfake videos from a recently proposed dataset, Deepfakes from Different Models (DFDM), derived from various Autoencoder models. The dataset comprises 6.450 Deepfake videos generated by five distinct models with variations in encoder, decoder, intermediate layer, input resolution, and compression ratio. This study formulates Deepfakes model attribution as a multiclass classification task, proposing a segment of VGG19 as a feature extraction backbone, known for its effectiveness in imagerelated tasks, while integrated a Capsule Network with a Spatio-Temporal attention mechanism. The Capsule module captures intricate hierarchies among features for robust identification of deepfake attributes. Additionally, the video-level fusion technique leverages temporal attention mechanisms to handle concatenated feature vectors, capitalizing on inherent temporal dependencies in deepfake videos. By aggregating insights across frames, our model gains a comprehensive understanding of video content, resulting in more precise predictions. Experimental results on the deepfake benchmark dataset (DFDM) demonstrate the efficacy of our proposed method, achieving up to a 4% improvement in accurately categorizing deepfake videos compared to baseline models while demanding fewer computational resources.

Index Terms—Deepfakes, Model Attribution, CapsuleNet.

Wasim Ahmad is with the Institute of Information Science, Academia Sinica, Taipei 11529, Taiwan (R.O.C) and Department of Computer Science, National Chengchi University, Taipei 116, Taiwan (R.O.C) and Social Networks Human-Centered Computing, Taiwan International Graduate Program, Academia Sinica, Taipei 11529, Taiwan (R.O.C) (E-mail: was_last@iis.sinica.edu.tw

Yan-Tsung Peng is with Department of Computer Science National Chengchi University, Taipei 116, Taiwan (R.O.C) (E-mail: ytpeng@cs.nccu.edu.tw).

Yuan-Hao Chang is with the Institute of Information Science, Academia Sinica, Taipei 11529, Taiwan (R.O.C) (E-mail: johnson@iis.sinica.edu.tw).

Gaddisa Olani Ganfure. is with Dire Dawa University, Ethiopia (E-mail: gaddisaolex@gmail.com).

Sarwar Khan is with the Research Center for Information Technology Innovation, Academia Sinica, Taipei 11529, Taiwan (R.O.C) and Department of Computer Science, National Chengchi University, Taipei 116, Taiwan (R.O.C) and Social Networks Human-Centered Computing, Taiwan International Graduate Program, Academia Sinica, Taipei 11529, Taiwan (R.O.C) (E-mail: sarwar@iis.sinica.edu.tw).

Sahibzada Adil Shahzad is with the Institute of Information Science, Academia Sinica, Taipei 11529, Taiwan (R.O.C) and Department of Computer Science, National Chengchi University, Taipei 116, Taiwan (R.O.C) and Social Networks Human-Centered Computing, Taiwan International Graduate Program, Academia Sinica, Taipei 11529, Taiwan (R.O.C) (E-mail: adilshah275@iis.sinica.edu.tw).

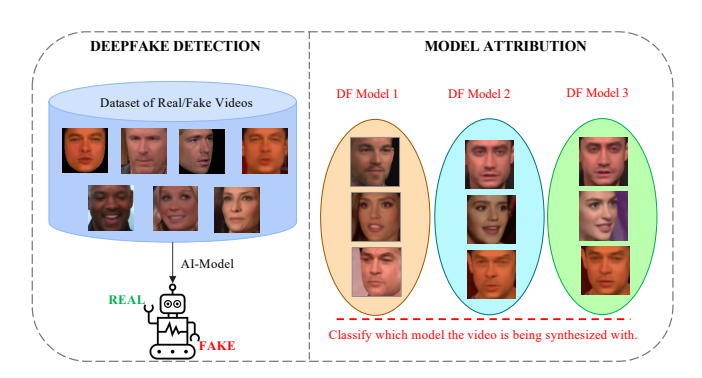


Fig. 1. In contrast to prevailing methods designed to differentiate between authentic and manipulated videos, Deepfake model attribution seeks to discern the specific generation model employed in a given DeepFake video. This process is instrumental in tracing the video's authorship and source.

I. Introduction

THE term "Deepfake," derived from 'deep learning' and 'fake,' commonly denotes AI-generated face-swap videos, wherein the faces of the original subject (the 'source') are replaced with those of another person (the 'target'). Generated using deep learning models with the same facial expressions as the source, these videos have become increasingly easy to produce with the advent of open-source generation tools [1]. The potential weaponizing of Deepfakes by malicious actors to manipulate identities and spread disinformation has raised widespread concerns [2].

In response, there has been a growing research interest in Deepfake detection methods current face forgery technologies encompass various techniques, including non-target face generation [2, 3], expression replay [4, 5], face replacement [6, 7] and attribute editing [8, 9].

Existing techniques often leverage visual/signal artifacts [10, 11, 12] or novel deep neural networks [13, 14, 15, 16]. Notable datasets of Deepfake videos have been curated, including Faceforensics++ [17], Deeperforensics-1.0 [18], DFDC [19], WildDeepfake [20] and Celeb-DF [21]. While state-of-the-art detection methods have shown promising performance on benchmark datasets, the specific methods employed in Deepfake creation are crucial for forensic analysis as shown in Figure 1. Knowing the synthesis model used can help narrow down potential users who have downloaded publicly available tools.

The model attribution problem, crucial for understanding the creation process of Deepfakes, has been explored in recent studies concerning Generative Adversarial Network (GAN)-

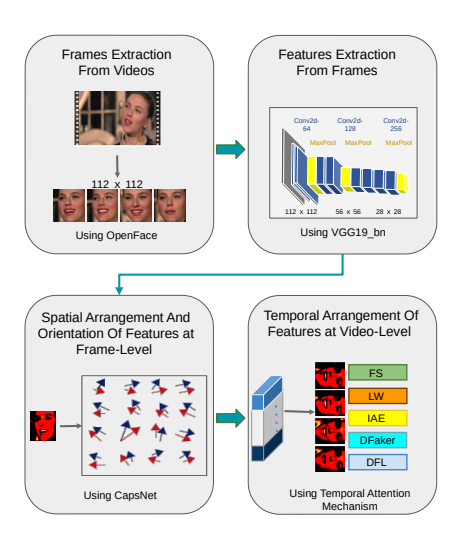


Fig. 2. General Overview of CapST: First, we extract the distinctive attributes of a set of video frames using VGG19. Subsequently, these resultant features are fed into the capsule module to delineate spatial configurations within each frame. At last, these refined features are directed into the video-level fusion module, thereby enabling the classification of the manipulated class to which the video pertains.

based models [22, 23, 24] as shown in Figure 3. However, the model attribution methods developed for GAN images are not directly applicable to face-swap Deepfake videos. This distinction presents a more challenging scenario, particularly because Autoencoder-based models, commonly used in Deepfake creation [25], attenuate high-frequency features in generated video frames, a characteristic on which previous methods for GAN model attribution rely. DFDM is generated using various autoencoder models, as illustrated in Table I. DFDM comprises five balanced categories of Deepfake videos, created through Facewap [26], with variations in the encoder, decoder, intermediate layer, and input resolution.

In this study, we introduce an innovative approach to address the challenge of model attribution by proposing an enhanced and lightweight model, which combines the power of Capsule Network [27] and a modified Spatio-Temporal Attention mechanism. Notably, this marks only the second attempt in this domain, following the work presented in [28] and shown in Figure 2. The key contributions of this study include:

- Proposal of a novel technique CapST, utilizing VGG19 as a backbone for features extraction, coupled with Capsule Network and Spatio-Temporal Attention, demonstrating superior performance compared to existing solutions.
- The versatility of our model extends beyond model attribution, making it applicable to a range of classification tasks.
- The proposed solution is resource-efficient, addressing concerns of resource utilization, as it is not densely configured which is critical for training large models.
- Experimental results showcase the effectiveness of our model in accurately handling the model attribution problem, achieving a performance improvement of up to 4%, while significantly reducing resource utilization to only 3.27 million parameters.

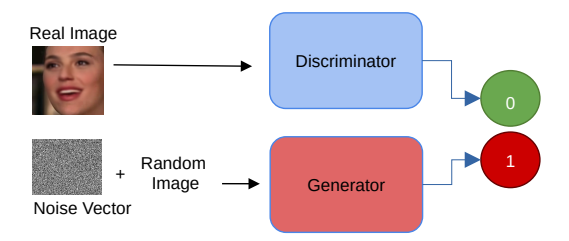


Fig. 3. The process of Generative Adversarial Networks (GANs) to produce lifelike and top-notch data involves training two neural networks, specifically a generator and a discriminator, within an adversarial framework.

II. BACKGROUND AND RELATED WORK

A. Video/Image Forgery Detection

In the early stages of face generation technologies, direct visual artifacts and inconsistencies in facial areas were common due to their uncontrollable characteristics. Image forgery detection efforts often leveraged statistical inconsistencies in faces or heads. For instance, [29] proposed Face X-ray, a method predicting blending boundaries in fake video frames. [30] employed adversarial learning to add perturbations to regions of interest, revealing vulnerabilities in current imagebased forgery detection. [31] tracked potential texture traces during image generation, performing well on multiple benchmarks. [32] introduced an Artifacts-Disentangled Adversarial Learning framework for accurate deepfake detection. Leveraging the Multi-scale Feature Separator (MFS) and Artifacts Cycle Consistency Loss (ACCL), our approach refines artifact estimation through pixel-level supervised training. [33] demonstrated good generalization abilities through intraconsistency within classes and inter-diversity between classes. However, with the advancement of DeepFake generation techniques, image-based detectors may fail to capture temporal inconsistencies across multiple frames, as early forgery generation technology showed obvious temporal inconsistency between frames. [34] also introduced a spatial and temporal level two-stream detection network, achieving significant improvements on post-processing compressed low-pixel videos. [35] proposed a temporal convolution network effective in extracting temporal features and improving generalization. [36] developed a forgery detection method capturing local spatiotemporal relations and inconsistencies in deepfake videos. [37] proposes AGLNet, aiming to improve deepfake detection by considering spatial and temporal correlations. AGLNet employs attention-guided LSTM modules to aggregate detailed information from consecutive video frames. [38] explore and adapt attention mechanisms for deepfake detection, specifically focusing on learning discriminative features that consider the temporal evolution of faces to identify manipulations. The research addresses the questions of how to use attention mechanisms and what type of attention is effective for deepfake detection. [39] introduces a neural Deepfake detector aiming to identify manipulative signatures in forged videos at both frame and sequence levels. Using a ResNet backbone with spatial and distance attention mechanisms, the model is trained as a classifier to detect forged content. [40] Introduced MSVT, a novel

Model	Input	Output	Encoder	Decoder	Variation
Faceswap (baseline)	64	64	4Conv+1Ups	3Ups+1Conv	/
Lightweight	64	64	3Conv+1Ups	3Ups+1Conv	Encoder
IAE	64	64	4Conv	4Ups+1Conv	Intermediate layers;Shared Encoder Decoder
Dfaker	64	128	4Conv+1Uns	3Uns+3Residual+1Conv	Decoder

TABLE I STRUCTURE OF DFDM DATASET [28]

Multiple Spatiotemporal Views Transformer with Local (LSV) and Global (GSV) views to extract detailed spatiotemporal information. Utilizing local-consecutive temporal views for LSV and a global-local transformer (GLT), MSVT effectively integrates multi-level features for comprehensive information mining. [41] proposed a dynamic difference learning method for precise spatio-temporal inconsistency in deepfake detection, employing a dynamic fine-grained difference capture module (DFDC-module) with self-attention and denoising, along with a multi-scale spatio-temporal aggregation module (MSA-module) for comprehensive information modeling. This approach extends 2D CNNs into dynamic spatio-temporal inconsistency capture networks. [42] Introduced ITSNet, an Interactive Two-Stream Network for cross-modality discriminant inconsistency representation. Utilizing DDCT for fine-grained clues and incorporating Short-term and Long-term Embedding Modules, ITSNet refines both local and long-range temporal inconsistency.

B. Popular Deepfake models and Datasets

DFL-H128

Recent strides in deepfake technology result from the advancement of sophisticated models and the availability of well-curated datasets. These instrumental components have significantly advanced the frontiers of deepfake synthesis, detection, and analysis. Earlier discussions highlighted a plethora of studies presenting outstanding AI models that exhibited superior performance across diverse datasets, as detailed in the subsequent section. However, a prevalent challenge among these models lies in their size and complexity, leading to heightened daily resource demands. The following section provides insights into renowned deepfake detection models and datasets, encompassing their resource consumption parameters. Refer to Table II for specific examples of these models and datasets.

1) DeepFake Models: XceptionNet [17] is a deep CNN architecture with high performance in deepfake detection, utilizing depthwise separable convolutions for fine-grained feature capture. DeepFakeTIMIT [43] specializes in audio-visual deepfake synthesis, combining audio and visual information. Ensemble Models combine predictions from diverse models, achieving robust deepfake detection. SqueezeNAS [44] is an automated design framework for compact models, optimizing for accuracy and efficiency. FWA-Net focuses on detecting facial warping artifacts using a two-stream architecture. Capsule-Forensics [14] utilizes capsule networks for forged image and video detection. MesoNet [16] is a lightweight CNN for mesoscopic-level detection. DFDNet [45] employs a two-stream architecture for spatiotemporal features.

TABLE II POPULAR DF MODELS, DATASETS AND ITS PARAMETERS

Input Resolution

Models	Datasets	Params(M)	
X-Ray [29]	FF++ UADFV CDF_v1,v2	20.8	
CNN+RNN [50]	FF++ UADFV CDF_v1,v2	36	
TSN [35]	FF++ UADFV CDF_v1,v2	26.6	
DSP-FWA [51]	FF++ UADFV CDF_v1,v2	21.4	
Two-stream [52]	FF++ UADFV CDF_v1,v2	23.9	
Meso4 [16]	FF++ UADFV CDF_v1,v2	28.0	
MesoInception4 [16]	FF++ UADFV CDF_v1,v2	28.6	
FWA [53]	FF++ UADFV CDF_v1,v2	25.6	
Xception-raw,c-23,c40 [17]	FF++ UADFV CDF_v1,v2	22.9	
Capsule [14]	FF++ UADFV CDF_v1,v2	3.9	
Multi-attentional [54]	FF++ UADFV CDF_v1,v2	19.5	
FTCN [35]	FF++ UADFV CDF_v1,v2	26.6	
RealForensics [51]	FF++ UADFV CDF_v1,v2	21.4	
ResVit [55]	FF++ DFD CDF_v1,v2	21.4	
Cross Eff_ViT [56]	DFDC	109	
Selim EffNet B7 [57]	DFDC	462	
Convolutional ViT [58]	DFDC	89	
Lipsync Matters [59]	FakeAVCeleb	35.97	
Multimodal [60]	FakeAVCeleb	33.6	

2) Datasets: FaceForensics++ [17] is a benchmark with over 1,000 manipulated facial videos. CelebA [46] provides a large celebrity image collection. DFDC Dataset [47] targets state-of-the-art deepfake video detection. Face2Face [48] manipulates facial expressions in videos. VoxCeleb Dataset [49] offers diverse audio-visual celebrity speech data. Deepfake-TIMIT [43] is tailored for audio-visual synthesis. FBDB [19] by Facebook provides a large-scale dataset for training and evaluation.

C. Model Attribution

Model attribution involves the crucial task of identifying the specific model employed in the generation of synthetic images or videos [22]. Within the domain of image manipulation, the pervasive use of Generative Adversarial Network (GAN) models has spurred numerous investigations [23, 61] into GAN model attribution, particularly concerning counterfeit images. These attribution methodologies aim to extract distinctive artificial markers left by diverse GAN models, employing multi-class classification techniques to attribute the specific GAN model used. However, until the work by Jia et al. [28], prior research had not concentrated on model attribution specifically for Deepfake face-swap videos. While GAN models are capable of producing Deepfakes, their effectiveness is often constrained to controlled settings with uniform lighting conditions [19]. Consequently, the generation of publicly available face-swap Deepfakes frequently relies on

Deepfake Autoencoder (DFAE) techniques. The feasibility of differentiating between various DFAE models for Deepfake attribution and the extent to which image-based GAN model attribution techniques are applicable to DFAE models in the video domain remain subjects warranting exploration. These inquiries are pivotal in advancing Deepfake model attribution, addressing research gaps, and enhancing our understanding of challenges in attributing models for face-swapping techniques. The exploration of attribution methodologies across generative models and their application to diverse video-generation techniques contributes to ongoing efforts in improving the reliability and robustness of model attribution in the evolving landscape of synthetic media [22, 23, 61, 28, 19].

III. CAPST ARCHITECTURE

This study emphasizes resource-efficient Deep Neural Network (DNN) design for targeted domains. Our CapST Model, detailed in this section, combines Capsule Network with Spatial and Temporal attention mechanisms for deepfake content analysis. Extracting frames, utilizing VGG_19_bn for feature extraction, and employing Capsule Network with MFM Activation and Spatial Attention, our algorithm enhances artifact detection. TAM ensures adaptive feature aggregation across frames, enhancing accuracy in deepfake classification (Algorithm 1).

A. Unveiling the intricacies of DF artifacts at frame-level

The architecture of our CapST model is depicted in Figure 4. We first extract N number of faces from each video in the dataset, i.e.,

$$V_i = I_{f1}, I_{f2}, \dots, I_{fN},$$
 (1)

where V_i represents the input video while I_{f1}, \ldots, I_{fN} represents the number of input frames we chose to consider for each video. After that, we pass these frames one by one to the VGG_19 network, where we extract the features of the input frame. We choose VGG_19bn as a feature extractor pretrained on [62] from the first-to-third Max-Pooling layer with a total of 26 layers. VGG_19bn is used as its performance is better throughout all the experiments than other CNN networks in this specific task. The extracted features are then passed through the Capsule Network as shown in Figure 5.

We divided each primary capsule into three sections, including the Max Feature Map (MFM) [63] Activation function with the combination of Batch Normalization and Spatial Attention Layer, statistical pooling layer, and a 1-dimensional CNN. The statistical pooling layer is considered efficacious for forensics tasks and can improve the performance of the network [64, 65] by making the network independent even if the dimension of the input images vary. This is why it is argued that this network is not task-oriented and can be applied to different tasks without redesigning the whole network from scratch.

The capsule module first passes the input features through the MFM activation function proposed in [63], which enables the network to become light and robust as it suppresses the low activation neurons in each primary capsule. The output of the MFM is then passed through a spatial attention layer to aggregate the frame features [66]. The Statistical pooling layer is then used to calculate the mean and variance of each filter/kernel, as shown below.

• Mean:
$$\mu_k = (1/H \times W - 1) \sum_{i=1}^H \sum_{j=1}^W I_k ij$$

• Variance:
$$\sigma_k^2 = (1/H \times W - 1) \sum_{i=1}^H \sum_{j=1}^W (I_k i j - \mu_k)^2$$

Here, the variable k denotes the index of the layer, while H and W represent the height and width of the filter, respectively. I refers to a two-dimensional array of filters. The outcome from the statistical layer lends itself well to 1D convolution. After traversing the ensuing 1D convolutional segment, the data undergoes dynamic routing to reach the output capsules. The ultimate outcome is determined based on the activation status of the output capsules. This process is followed by the presence of five output capsules designated for the purpose of multi-class classification, depicted in Fig 5. The ultimate output is derived from the activation patterns exhibited by the output capsules.

B. Unveiling the intricacies of DF artifacts at video-level

The outcomes of each individual frame, as shown in Equation 1, after undergoing each step of frame-level fusion, are subsequently combined for the specific number of frames representing a single video instance as shown in Equation 2.

$$V_o = O_{f1}, O_{f2}, \dots, O_{fN},$$
 (2)

where V_o represents the output video while O_{f1}, \ldots, O_{fN} represents the number of output frames from 1 upto Nwe chose to consider for each video. While prior research on video-level Deepfake detection mainly fused multi-frame characteristics by averaging network predictions (score fusion) [53, 16, 14, 28, 67], we have chosen to enhance classification performance by employing a temporal attention map (TAM) for adaptive feature aggregation across frames. This approach involves concatenating frame features from N faces to create multi-frame representations, which are then fused into an adaptive representation using a TAM-a structure akin to SENet [68]. The TAM utilizes the ReLU activation function along with two fully connected layers, and its output is subsequently fed into a fully connected layer for classification purposes, yielding class probabilities for the five Deepfake categories. The network is trained using the cross-entropy function. Differing from conventional Deepfake detection techniques, our approach incorporates an attention mechanism harnessing the capabilities of the Capsule Network in frame-level fusion to extract differences for model attribution subtly. In contrast to prior fingerprint-based GAN model attribution studies, the CapST takes the entire facial content as input rather than designing supplementary artifacts for multi-classification tasks, enabling effective and automatic learning of discrepancies among distinct Deepfakes.

After traversing through the stages of frame-level fusion, the outcome of each frame is amalgamated over a specific number

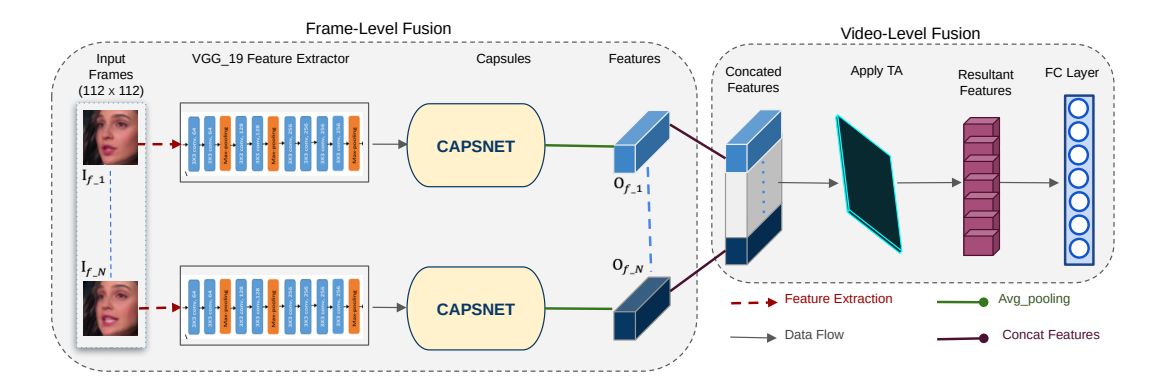


Fig. 4. CapST Main architecture

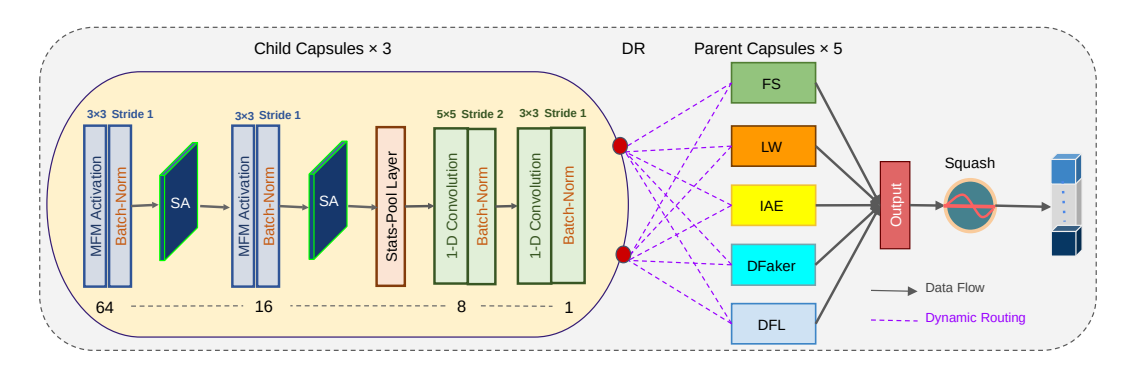


Fig. 5. Capsule Module

of frames representing an individual video. While prior investigations in the domain of video-level Deepfake detection often amalgamated multi-frame attributes by computing an average of network predictions (score fusion), our enhancement to classification efficacy involves the deployment of a temporal attention map for the adaptive accumulation of attributes across diverse frames. Initially, the features of N faces' frames are concatenated to shape multi-frame representations, which are subsequently melded using the temporal attention map. This attention map shares a similar structure with SENet [68] and employs the ReLU activation function alongside two fully connected layers. The resulting output is then channeled through a fully connected layer tailored for classification, producing probabilities for the five Deepfake categories. Training the neural network encompasses the utilization of the cross-entropy function. In contrast to existing techniques, our strategy harnesses the attention mechanism of the Capsule Network to extract variations in model attribution at the frame level delicately. Diverging from fingerprint-based GAN model attribution studies, the CapST approach accepts entire facial content as input, obviating the need for supplementary artifacts and allowing for effective, automatic assimilation of differences among distinct Deepfakes.

Algorithm 1 CapST Algorithm

Require: Dataset of videos with N frames each **Ensure:** Probabilities for each DF video's class

- 1: for each video V in the dataset do
- 2: **for** each frame I_f in N faces extracted from V **do**
- 3: Extract features from I_f using VGG_19_bn
- 4: end for
- 5: **for** each frame feature **do**
- 6: Pass through MFM Activation Function
- 7: Apply Batch Normalization
- 8: Pass through Spatial Attention MAP (SAM)
- 9: Compute mean (μ_k) and variance (σ_k^2) (StatsPool)
- 10: Extract final features using a 1D CNN segment
- 11: end for
- 12: end for
- 13: Initialize: Temporal Attention Map (TAM)
- 14: **for** each video V **do**
- 15: Concatenate features for multi-frame representations
- 16: Pass through Temporal Attention Map (TAM)
- 17: Pass through fully connected layer for classification
- 18: end for
- 19: return Class probabilities for each DF video's class

IV. EXPERIMENTS AND RESULTS

A. DFDM Dataset

The Deepfakes from Different Models (DFDM) dataset, highlighted by [28], stands out in the realm of Deepfakes due to its unique features. Filling the void of labeled Deepfakes from diverse models, the authors introduced the DFDM dataset. Notably, Autoencoder architectures, widely used in public Deepfakes [19, 20] were emphasized. The study employed the Facewap open-source software [26] and selected DFAE models from DeepFaceLab [69]. Five models, including Faceswap, Lightweight, IAE [26], Dfaker [70], and DFL-H128 [71], were meticulously chosen, ensuring subtle distinctions. Genuine videos were drawn from the Celeb-DF dataset [21], featuring 590 YouTube interviews with 59 celebrities, ensuring diverse content. Facial features were extracted using the S3FD detector [72] and FAN face aligner [73]. Each model underwent 100,000 training iterations, generating Deepfake videos in MPEG4.0 format. Varying H.264 compression rates (CRF 0, 10, 23) resulted in 6,450 Deepfakes. Figure 7 illustrates facial differences among Deepfakes created by these models from the same dataset, highlighting model-specific artifacts.

B. Experimental Setting

Before conducting our experiments, we divided the DFDM dataset into training and testing sets following the guidelines provided by [28], with a ratio of 70% for training and 30% for testing. To extract frames from each video in the dataset, we utilized the OpenFace open-source library [74], known for its accuracy and reliability. The extracted frames were saved in PNG format with a dimension of 112×112 pixels. By using a lower dimension, we aimed to reduce the computational resources required for training our model, which is one of the main objectives of this study. To ensure a balanced distribution of faces in frame selection, we employed periodic sampling to select 10 frames from each video for our proposed approach. Our experimental results indicate a clear performance improvement when increasing the number of frames from 1 to 10, while the performance becomes stable beyond 10 frames. Thus, the network takes the cropped faces with dimensions of $112 \times 112 \times 3 \times 10$ as input. For training the network, we used the SGD optimizer with a weight decay of 5×10^{-4} and a momentum of 0.9. The learning rate was set to 0.01 throughout the entire training process. A batch size of 10 was employed, and the training was conducted for 300 epochs. We adapted the cross-entropy loss function to suit the requirements of our specific task, which involved the classification of five manipulated classes. This task, focused on model attribution, required a modification of the standard binary cross-entropy loss. Our customized loss function is formulated as:

$$L(\mathbf{y}, \hat{\mathbf{y}}) = -\sum_{i=1}^{5} y_i \cdot \log(\hat{y}_i)$$

Here, y represents the true label vector with five elements, and \hat{y} is the predicted probability vector for each of the five classes. This tailored approach allowed us to effectively train our model for the nuanced task of classifying instances into one of the five manipulated classes.

C. Results Comparison With Existing Methods

Table III compares our model and various state-of-theart methods, including attention-based and other classification approaches. Our model stands out, surpassing all other contenders in terms of overall accuracy. This success underscores the superior classification prowess of our approach. While some of the competing models leverage skip connections and more intricate architectures, our choice of a simple VGG19 model without residuals yields exceptional results. These models may exhibit enhanced performance in specific classes due to their utilization of models that uses skip connections, which can sometimes perform better in specific condition/classes, but their overall effectiveness falls short of overall improvement. It's important to acknowledge that, in general, ResNet has demonstrated superior accuracy compared to VGG19 across diverse image recognition tasks, particularly on large-scale challenges like ImageNet. However, for our specific problem domain and dataset, VGG19 has proven to be a robust performer. Ultimately, the decision to opt for ResNet or VGG19 should be made thoughtfully, considering the specific demands and nuances of each task at hand. To conclude, we carefully conducted several experiments and observed that VGG_19_bn, combined with Capsule Network, can achieve better performance, as shown in Figure 6.

D. Comparing Our Results to DMA-STA Reproduced Results

While the initial performance of DMA-STA [28] was promising, our model demonstrated significant superiority after applying our custom settings, as shown in Table V. However, we have difficulty replicating their outcomes using their GitHub repository's experimental configurations. Our machine's limited GPU memory prevented us from using their settings. To optimize model efficiency and resource usage, we adjusted the original settings that involved image dimensions from the video dataset and batch size. The original DMA-STA experiments employed Titan XP GPUs [78], but we had access to a single GPU with 12 Gigabytes of memory. To ensure a fair comparison, we adapted the experimental parameters to reproduce DMA-STA's results on our machine. Specifically, we reduced image dimensions from 300×300 to 112×112 and the batch size from 20 to 10 while keeping other settings unchanged. For a detailed explanation of the rationale behind these adjustments, please refer to Section V-A.

E. Parameters Comparison with DMA-STA

Incorporating ResNet for feature extraction, renowned for its efficient parameter utilization, the DMA-STA network takes

TABLE III
COMPARISON OF CAPST MODEL WITH DIFFERENT METHODS (ACC%). THE BEST SCORE IS MARKED IN BOLD.

Method	FaceSwap	LightWeight	IAE	Dfaker	DFL-H128	Average
MesoInception [16]	6.98	2.33	79.07	79.07	4.65	20.93
XceptionNet [17]	0.77	0.00	12.40	12.40	19.38	20.93
R3D [15]	27.13	25.58	15.5	20.16	18.61	21.40
DSP-FWA [53]	17.05	7.75	43.41	40.31	8.87	23.41
GAN Fingerprint [61]	20.16	22.48	54.26	21.71	26.36	28.99
DFT-spectrum [75]	99.92	3.26	0.23	27.21	48.91	35.91
Capsule [14]	32.56	42.64	69.77	73.64	58.91	55.50
SAM+FA [76]	64.34	42.64	76.61	74.42	79.07	66.82
ResNet-50 [77]	54.84	57.36	70.54	89.92	70.54	68.02
CBAM [66]	52.42	63.57	69.77	84.50	74.42	68.53
SAM+Ave	58.87	51.16	76.74	80.62	79.07	68.84
DMA-STA [28]	63.57	58.91	66.67	82.95	87.60	71.94
CapST[Ours]	77.69	53.84	60.76	93.07	92.30	75.54

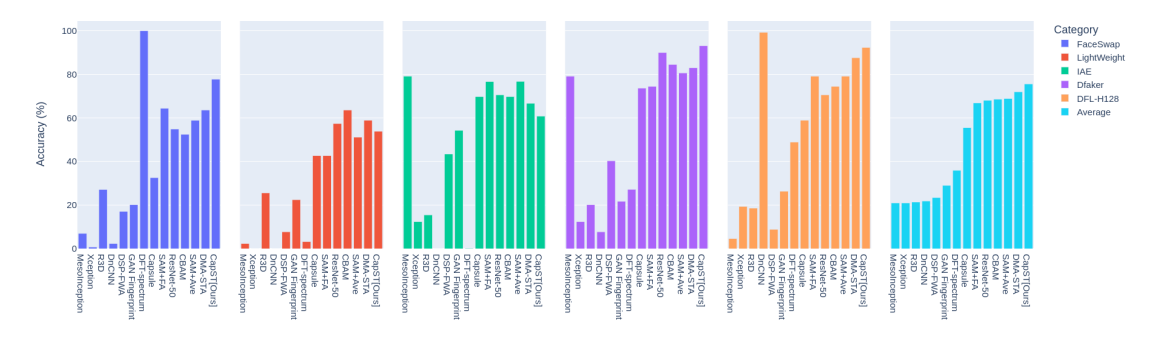


Fig. 6. Results Comparison of CapST Model Against Existing Methods

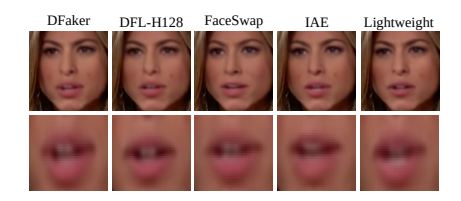


Fig. 7. DFDM Example: Generated By Different Encoders

a step further by integrating two modules known as Spatial-Temporal attention. In the initial segment of these modules, frame-level characteristics are derived from N cropped faces via the utilization of the Spatial Attention Map (SAM). This process inherently captures elevated-level representations, facilitated by utilizing the lightweight and versatile convolutional block attention module introduced by [66]. Moreover, the Temporal Attention Map (TAM) is harnessed to adaptively consolidate attributes from diverse frames. Integrating these intricate modules leads to a substantial augmentation in the model's parameter count, culminating in a total of 23.520 million parameters. In contrast, our model not only surpasses the performance of the existing one but also significantly reduces the number of parameters to a mere 3.27 million, which is almost eight times smaller than the current model's parameter count. We also consider training time an essential factor, as training huge models that require substantial time for learning data might be undesirable in the future. Therefore, we have designed our model to take less time to train while still outperforming existing models in this specific task, as

demonstrated in Table VI. This approach ensures efficiency in training without compromising performance.

V. DISCUSSION

The CapST module's robust capabilities extend beyond mere computational resource reduction, encompassing the simultaneous maintenance of high performance. Our approach unfolds in four distinct phases. Initially, frames are extracted from each video. Subsequently, these frames are subjected to feature extraction using the VGG19 model. The decision to favor VGG19 over ResNet stems from its demonstrated superior performance when integrated with the Capsule network, a conclusion drawn from meticulous experimentation involving both architectures. Notably, despite ResNet's intrinsic parameter efficiency compared to VGG19, a deliberate choice is made to exclusively engage the first three Maxpooling layers of VGG19 (which spans 26 layers), effectively constraining the overall parameter count during the training process. Moving forward, the extracted features are channeled into the Capsule module, enriching each input video frame with spatial characteristics. Lastly, the video-level fusion procedure comes into play, culminating in successfully classifying the video into its pertinent category of interest. The distinguishing factor between CapST and prior studies lies in our deliberate efforts to reduce image dimensions, batch size, and training time. These considerations, tailored to the constraints of FPGAbased hardware, yield a substantial solution to address the challenge of classifying deepfake content. Further elaboration is provided in Section V-A.

TABLE IV
RESOURCES AND PERFORMANCE COMPARISON OF CAPST MODEL
AGAINST DIFFERENT MODELS (ACC%). THE BEST ONE IS MARKED
IN BOLD

Model	Training Time	Params	Avg: Acc(%)
MobileNet-V1 [79]	33	3.21	21.69
EfficientNet [81]	90	4.01	71.69
ResNet-50 [77]	116	23.52	60.92
ResNet-101 [77]	203	42.51	60.61
ResNet-152 [77]	268	57.03	60.46
XceptionNet [82]	120	20.81	38.61
InceptionNet [83]	126	6.27	42.76
MobileNet-V2 [80]	118	2.23	21.69
CapST[Ours]	112	3.27	75.54

¹ Training Time* is presented in Minutes.

A. Ablation Study

We made several modifications to the baseline model aimed at reducing computational demands while simultaneously enhancing performance in video classification, as illustrated in Table IV. To evaluate the efficacy of these changes, we substituted the Capsule Network with various existing models, carrying out these experiments under uniform settings and environmental conditions. For every experiment, the input frame dimensions were fixed at 112×112 , and we opted for a batch size of 10 for both the training and testing phases. This choice was due to hardware limitations that restricted us from employing batch sizes greater than 10. Each experiment was executed for 300 epochs, and the results were analyzed. As depicted in Figure 8, MobileNet [79] exhibited the shortest training time of 33 minutes and a relatively low parameter count of 3.21 million during the training process. However, its performance was notably low, registering at 21.69%. Similarly, MobileNet-V2 [80] possessed fewer training parameters, yet its training time was comparatively higher, and its performance is the same as that of MobileNet [79], which was subpar. EfficientNet [81] achieved a relatively higher performance score of 71.69%, supported by a modest training parameter count of 4.01 million and a training duration of 90 minutes. However, compared to our proposed model, its overall performance remains inferior. Compared to all other models, our proposed model exhibited an appropriate training time and an impressively lower parameter count, outperforming all others. This model's performance also surpassed that of its counterparts. The rationale underpinning these modifications is elaborated upon in the subsequent explanation.

B. Discussions

1) Dimension of Images: The dimension of images in a dataset significantly impacts the size of the model, particularly in deep learning architectures, as it is closely tied to the number of parameters required for effective data representation. This influence is evident in various aspects of the model's architecture. Image dimensions directly affect pixel count, where larger images, such as 256×256 compared to 64×64 , demand a greater number of parameters for

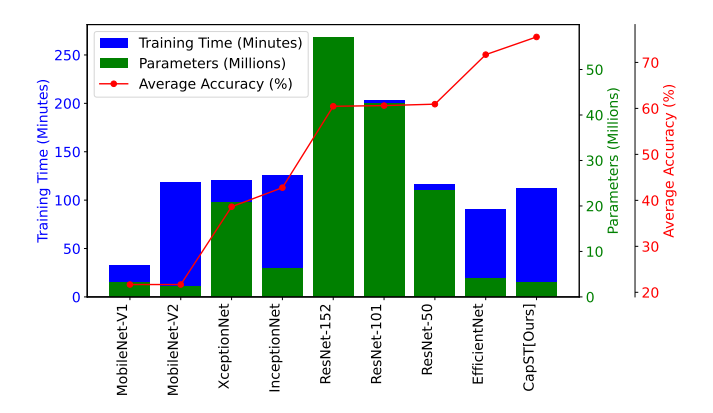


Fig. 8. Resources/Performance Comparison of CapST against state-of-the-art Models on DFDM Dataset

processing. The input image size dictates the dimensions of convolutional layers in architectures like CNNs, and larger images may necessitate more filters, thereby increasing the number of parameters. The size of the image affects the number of units in dense layers, with larger images potentially requiring more units and leading to an increase in parameters. Larger images might need additional pooling layers, impacting model size by reducing spatial dimensions. Memory needs also increase with larger images, influencing the model's feasibility. Processing larger images increases floating-point operations, extending both training and inference times. Striking a balance between model size and detail is crucial, as opting for smaller image dimensions helps reduce parameters, memory usage, and computational costs. However, finding the right balance is essential, as overly reducing size may sacrifice crucial details, ultimately harming the model's performance. Therefore, decisions regarding image dimensions require careful consideration of the trade-offs between size and performance in deep-learning tasks.

- 2) Effect of Batch size: The optimal batch size in deep learning depends on the task, hardware, and dataset size. There is no universal answer, as larger batches accelerate GPU training but may overfit, while smaller batches enhance generalization, crucial for small datasets. Hardware constraints, especially memory limitations, must be considered; large batches demand more memory, challenging on limited GPU/system memory. Small batches are memory-efficient, suitable for restricted resources and transfer learning. Batch noise is a factor; large batches smooth noisy data, and smaller batches explore the loss landscape effectively. The choice depends on specific needs and resources, requiring experimentation to balance efficiency and generalization. In our experiments, a smaller batch size was chosen due to our dataset and limited hardware.
- 3) Effect of Training Time: Training time significantly impacts various aspects of deep neural networks, including computational costs, iterative improvements, deployment, and time-sensitive applications. Faster training is crucial for cost reduction, swift testing, and quicker model updates, benefiting both experimental exploration and real-world use. Balanc-

² Parameters* are presented in Millions

ing efficiency and accuracy is essential, and the appropriate approach depends on the specific use case and available resources, with techniques like efficient architectures and hyperparameter optimization contributing to faster training.

4) Effect of parameters on FPGA (Field-Programmable Gate Array) hardware: The Deep Learning model's parameter count significantly affects FPGA hardware, impacting resource use, edge device deployment, computation time, power consumption, parallelism, reprogramming speed, memory bandwidth, and training time. To optimize FPGA deployment, a balance is crucial between model complexity, resource constraints, and performance requirements. Efficient model design, pruning, quantization, and hardware-aware optimization maximize FPGA-based Deep Learning accelerator potential, requiring careful parameter choice for optimal performance and resource utilization.

VI. CONCLUSION

In summary, our research introduces a state-of-the-art lightweight model designed for accurate model attribution. Utilizing Convolutional Neural Network (CNN) for efficient feature extraction and a Capsule Network (CapsNet) for intricate hierarchies among features for not only identifying but robustly distinguishes deepfake attributes. Video-level fusion, acting as a temporal attention mechanism, enhances the model's capabilities by effectively leveraging temporal dependencies, resulting in a significant improvement in predictive accuracy. Empirical validation on a comprehensive deepfake dataset confirms the effectiveness and superiority of our approach. Results demonstrate a notable performance boost compared to the baseline model, while also addressing computational costs, crucial for real-world applicability and scalability. Amidst the escalating threat of deepfake videos, our method stands out as an innovative and timely contribution to enhanced detection and prevention strategies. This research lays the foundation for future advancements, taking a proactive stance against the challenges posed by the proliferation of synthetic media.

VII. ACKNOWLEDGEMENTS

This work was supported in part by National Science and Technology Council under grant nos. 112-2223-E-001-001, 111-2221-E-001-013-MY3, 111-2923-E-002-014-MY3, and 112-2927-I-001-508 and Academia Sinica under grant no. AS-IA-111-M01.

REFERENCES

[1] Siwei Lyu. "Deepfake detection: Current challenges and next steps". In: 2020 IEEE international conference on multimedia & expo workshops (ICMEW). IEEE. 2020, pp. 1–6.

TABLE V
COMPARISON WITH DMA-STA REPRODUCED RESULTS. THE BEST SCORE IS MARKED IN BOLD.

Method	lr	FS	LW	IAE	Dfake	r DFL	Avg
DMA-STA* [28]	$\begin{array}{ c c } 1\times \\ 10^{-2} \end{array}$	53.84	48.46	61.53	76.92	63.84	60.92
CapST: Orig_Caps	$\begin{array}{ c c } 1 \times \\ 10^{-4} \end{array}$	70.00	40.00	73.07	90.00	83.84	71.53
CapST: Orig_Caps	$\begin{vmatrix} 1 \times \\ 10^{-2} \end{vmatrix}$		38.46	76.92	87.69	91.53	73.38
CapST: MFM_5×5	$\begin{array}{ c c } 1 \times \\ 10^{-2} \end{array}$		42.30	73.84	90.76	91.53	74.15
CapST: MFM_3×3	$\begin{array}{ c c } 1 \times \\ 10^{-2} \end{array}$	77.69	53.84	60.76	93.07	92.30	75.54

¹ DMA-STA* reproduced results of the baseline method on our hardware.
² Ir, FS, LW and DFL represent Learning Rate, FaceSwap, Lightweight and DFL-H128, respectively

TABLE VI
PARAMETERS AND TRAINING TIME COMPARISON OF DMA-STA AND
CAPST MODELS ON RTX-3080TI

Index	Model Layers	Params(Millions)	Training Time(Minutes
		DMA-STA [28]	
0	Conv2D	9408	
1	BatchNorm	128	
2	Layer 1-4	23500064	0.5025×300
3	TA-FC0	50	
4	TA-FC1	50	
5	TA-FC	10245	
	Total	23.52	150.75
		CapsT [Ours]	
0	VGG	2328330	
1	CapsNet×3	942027	
2	TA-FC0	50	0.373×300
3	TA-FC1	50	
4	TA-FC	2565	
	Total	3.273	111.9

¹ Training Time* is calculated for 300 epochs in each experiment, as mentioned in the table above.

- [2] Taesung Park et al. "Contrastive learning for unpaired image-to-image translation". In: Computer Vision–ECCV 2020: 16th European Conference, Glasgow, UK, August 23–28, 2020, Proceedings, Part IX 16. Springer. 2020, pp. 319–345.
- [3] Tero Karras et al. "Analyzing and improving the image quality of stylegan". In: *Proceedings of the IEEE/CVF conference on computer vision and pattern recognition*. 2020, pp. 8110–8119.
- [4] Egor Burkov et al. "Neural head reenactment with latent pose descriptors". In: *Proceedings of the IEEE/CVF conference on computer vision and pattern recognition*. 2020, pp. 13786–13795.
- [5] Linsen Song et al. "Pareidolia face reenactment". In: Proceedings of the IEEE/CVF Conference on Computer Vision and Pattern Recognition. 2021, pp. 2236–2245.
- [6] Shruti Agarwal and Hany Farid. "Detecting deep-fake videos from aural and oral dynamics". In: *Proceedings* of the IEEE/CVF conference on computer vision and pattern recognition. 2021, pp. 981–989.

 $^{^3}$ 5 \times 5 and 3 \times 3 are kernal sizes

- [7] Yuhao Zhu et al. "One shot face swapping on megapixels". In: *Proceedings of the IEEE/CVF conference on computer vision and pattern recognition*. 2021, pp. 4834–4844.
- [8] Chaoyou Fu et al. "High-fidelity face manipulation with extreme poses and expressions". In: *IEEE Transactions on Information Forensics and Security* 16 (2021), pp. 2218–2231.
- [9] Zhiliang Xu et al. "Facecontroller: Controllable attribute editing for face in the wild". In: *Proceedings of the AAAI Conference on Artificial Intelligence*. Vol. 35. 4. 2021, pp. 3083–3091.
- [10] Luca Guarnera, Oliver Giudice, and Sebastiano Battiato. "Deepfake detection by analyzing convolutional traces". In: Proceedings of the IEEE/CVF conference on computer vision and pattern recognition workshops. 2020, pp. 666–667.
- [11] Trisha Mittal et al. "Emotions don't lie: An audio-visual deepfake detection method using affective cues". In: *Proceedings of the 28th ACM international conference on multimedia.* 2020, pp. 2823–2832.
- [12] Yuezun Li and Siwei Lyu. "Exposing deepfake videos by detecting face warping artifacts". In: *arXiv preprint arXiv:1811.00656* (2018).
- [13] Minha Kim, Shahroz Tariq, and Simon S Woo. "Fretal: Generalizing deepfake detection using knowledge distillation and representation learning". In: *Proceedings of the IEEE/CVF conference on computer vision and pattern recognition*. 2021, pp. 1001–1012.
- [14] Huy H Nguyen, Junichi Yamagishi, and Isao Echizen. "Capsule-forensics: Using capsule networks to detect forged images and videos". In: ICASSP 2019-2019 IEEE International Conference on Acoustics, Speech and Signal Processing (ICASSP). IEEE. 2019, pp. 2307–2311.
- [15] Oscar De Lima et al. "Deepfake detection using spatiotemporal convolutional networks". In: *arXiv* preprint *arXiv*:2006.14749 (2020).
- [16] Darius Afchar et al. "Mesonet: a compact facial video forgery detection network". In: 2018 IEEE international workshop on information forensics and security (WIFS). IEEE. 2018, pp. 1–7.
- [17] Andreas Rossler et al. "Faceforensics++: Learning to detect manipulated facial images". In: *Proceedings of the IEEE/CVF international conference on computer vision*. 2019, pp. 1–11.
- [18] Liming Jiang et al. "Deeperforensics-1.0: A large-scale dataset for real-world face forgery detection". In: *Proceedings of the IEEE/CVF conference on computer vision and pattern recognition.* 2020, pp. 2889–2898.
- [19] Brian Dolhansky et al. "The deepfake detection challenge (dfdc) preview dataset". In: *arXiv* preprint *arXiv*:1910.08854 (2019).
- [20] Bojia Zi et al. "Wilddeepfake: A challenging real-world dataset for deepfake detection". In: *Proceedings of* the 28th ACM international conference on multimedia. 2020, pp. 2382–2390.

- [21] Yuezun Li et al. "Celeb-df: A large-scale challenging dataset for deepfake forensics". In: *Proceedings of the IEEE/CVF conference on computer vision and pattern recognition*. 2020, pp. 3207–3216.
- [22] Sharath Girish et al. "Towards discovery and attribution of open-world gan generated images". In: *Proceedings of the IEEE/CVF International Conference on Computer Vision*. 2021, pp. 14094–14103.
- [23] Ning Yu, Larry S Davis, and Mario Fritz. "Attributing fake images to gans: Learning and analyzing gan finger-prints". In: *Proceedings of the IEEE/CVF international conference on computer vision*. 2019, pp. 7556–7566.
- [24] Michael Goebel et al. "Detection, attribution and localization of gan generated images". In: *arXiv* preprint *arXiv*:2007.10466 (2020).
- [25] Brian Dolhansky et al. "The deepfake detection challenge (dfdc) dataset". In: *arXiv* preprint *arXiv*:2006.07397 (2020).
- [26] deepfakes. *Faceswap*. https://github.com/deepfakes/faceswap. 2017.
- [27] Sara Sabour, Nicholas Frosst, and Geoffrey E Hinton. "Dynamic routing between capsules". In: *Advances in neural information processing systems* 30 (2017).
- [28] Shan Jia, Xin Li, and Siwei Lyu. "Model attribution of face-swap deepfake videos". In: 2022 IEEE International Conference on Image Processing (ICIP). IEEE. 2022, pp. 2356–2360.
- [29] Lingzhi Li et al. "Face x-ray for more general face forgery detection". In: *Proceedings of the IEEE/CVF conference on computer vision and pattern recognition*. 2020, pp. 5001–5010.
- [30] Haitao Zhang et al. "A local perturbation generation method for gan-generated face anti-forensics". In: *IEEE Transactions on Circuits and Systems for Video Technology* 33.2 (2022), pp. 661–676.
- [31] Jiachen Yang et al. "MSTA-Net: Forgery detection by generating manipulation trace based on multi-scale self-texture attention". In: *IEEE transactions on circuits and systems for video technology* 32.7 (2021), pp. 4854–4866.
- [32] Xin Li et al. "Artifacts-disentangled adversarial learning for deepfake detection". In: *IEEE Transactions on Circuits and Systems for Video Technology* 33.4 (2022), pp. 1658–1670.
- [33] Han Chen et al. "Learning Features of Intra-Consistency and Inter-Diversity: Keys Toward Generalizable Deepfake Detection". In: *IEEE Transactions on Circuits and Systems for Video Technology* 33.3 (2022), pp. 1468–1480.
- [34] Juan Hu et al. "Detecting compressed deepfake videos in social networks using frame-temporality two-stream convolutional network". In: *IEEE Transactions on Circuits and Systems for Video Technology* 32.3 (2021), pp. 1089–1102.
- [35] Yinglin Zheng et al. "Exploring temporal coherence for more general video face forgery detection". In: *Proceedings of the IEEE/CVF international conference on computer vision*. 2021, pp. 15044–15054.

- [36] Ipek Ganiyusufoglu et al. "Spatio-temporal features for generalized detection of deepfake videos". In: *arXiv* preprint arXiv:2010.11844 (2020).
- [37] Zhibing Wang et al. "Attention Guided Spatio-Temporal Artifacts Extraction for Deepfake Detection". In: *Chinese Conference on Pattern Recognition and Computer Vision (PRCV)*. Springer. 2021, pp. 374–386.
- [38] Abhijit Das, Srijan Das, and Antitza Dantcheva. "Demystifying attention mechanisms for deepfake detection". In: 2021 16th IEEE International Conference on Automatic Face and Gesture Recognition (FG 2021). IEEE. 2021, pp. 1–7.
- [39] Yunzhuo Chen et al. "Deepfake Detection with Spatio-Temporal Consistency and Attention". In: 2022 International Conference on Digital Image Computing: Techniques and Applications (DICTA). IEEE. 2022, pp. 1–8.
- [40] Yang Yu et al. "MSVT: Multiple Spatiotemporal Views Transformer for DeepFake Video Detection". In: *IEEE Transactions on Circuits and Systems for Video Technology* (2023).
- [41] Qilin Yin et al. "Dynamic Difference Learning with Spatio-temporal Correlation for Deepfake Video Detection". In: *IEEE Transactions on Information Forensics and Security* (2023).
- [42] Jianghao Wu et al. "Interactive Two-Stream Network across Modalities for Deepfake Detection". In: IEEE Transactions on Circuits and Systems for Video Technology (2023).
- [43] Burak Bekci, Zahid Akhtar, and Hazım Kemal Ekenel. "Cross-dataset face manipulation detection". In: 2020 28th Signal Processing and Communications Applications Conference (SIU). IEEE. 2020, pp. 1–4.
- [44] Mingyu Ding et al. "Hr-nas: Searching efficient highresolution neural architectures with lightweight transformers". In: Proceedings of the IEEE/CVF Conference on Computer Vision and Pattern Recognition. 2021, pp. 2982–2992.
- [45] Xiaoming Li et al. "Blind face restoration via deep multi-scale component dictionaries". In: Computer Vision–ECCV 2020: 16th European Conference, Glasgow, UK, August 23–28, 2020, Proceedings, Part IX 16. Springer. 2020, pp. 399–415.
- [46] Ziwei Liu et al. "Deep learning face attributes in the wild". In: *Proceedings of the IEEE international conference on computer vision*. 2015, pp. 3730–3738.
- [47] B Dolhansky et al. "The DeepFake detection challenge dataset.(2020)". In: *ArXiv: abs* (2006).
- [48] Justus Thies et al. "Face2face: Real-time face capture and reenactment of rgb videos". In: *Proceedings of the IEEE conference on computer vision and pattern recognition.* 2016, pp. 2387–2395.
- [49] Arsha Nagrani, Joon Son Chung, and Andrew Zisserman. "Voxceleb: a large-scale speaker identification dataset". In: *arXiv preprint arXiv:1706.08612* (2017).
- [50] Alexandros Haliassos et al. "Lips don't lie: A generalisable and robust approach to face forgery detection". In: Proceedings of the IEEE/CVF conference on computer vision and pattern recognition. 2021, pp. 5039–5049.

- [51] Du Tran et al. "Video classification with channel-separated convolutional networks". In: *Proceedings of the IEEE/CVF International Conference on Computer Vision*. 2019, pp. 5552–5561.
- [52] Peng Zhou et al. "Two-stream neural networks for tampered face detection". In: 2017 IEEE conference on computer vision and pattern recognition workshops (CVPRW). IEEE. 2017, pp. 1831–1839.
- [53] Yuezun Li and Siwei Lyu. "Exposing DeepFake Videos By Detecting Face Warping Artifacts". In: IEEE Conference on Computer Vision and Pattern Recognition Workshops (CVPRW). 2019.
- [54] Hanqing Zhao et al. "Multi-attentional deepfake detection". In: Proceedings of the IEEE/CVF conference on computer vision and pattern recognition. 2021, pp. 2185–2194.
- [55] Wasim Ahmad et al. "ResViT: A Framework for Deepfake Videos Detection". In: *International journal of electrical and computer engineering systems* 13.9 (2022), pp. 807–813.
- [56] Davide Alessandro Coccomini et al. "Combining efficientnet and vision transformers for video deepfake detection". In: *Image Analysis and Processing–ICIAP* 2022: 21st International Conference, Lecce, Italy, May 23–27, 2022, Proceedings, Part III. Springer. 2022, pp. 219–229.
- [57] Selim Seferbekov. DFDC 1st place solution. 2020.
- [58] Deressa Wodajo and Solomon Atnafu. "Deepfake video detection using convolutional vision transformer". In: arXiv preprint arXiv:2102.11126 (2021).
- [59] Sahibzada Adil Shahzad et al. "Lip Sync Matters: A Novel Multimodal Forgery Detector". In: 2022 Asia-Pacific Signal and Information Processing Association Annual Summit and Conference (APSIPA ASC). IEEE. 2022, pp. 1885–1892.
- [60] Ammarah Hashmi et al. "Multimodal Forgery Detection Using Ensemble Learning". In: 2022 Asia-Pacific Signal and Information Processing Association Annual Summit and Conference (APSIPA ASC). 2022, pp. 1524–1532. DOI: 10.23919/APSIPAASC55919.2022.9980255.
- [61] Francesco Marra et al. "Do gans leave artificial fingerprints?" In: 2019 IEEE conference on multimedia information processing and retrieval (MIPR). IEEE. 2019, pp. 506–511.
- [62] Olga Russakovsky et al. "Imagenet large scale visual recognition challenge". In: *International journal of computer vision* 115 (2015), pp. 211–252.
- [63] Xiang Wu et al. "A light CNN for deep face representation with noisy labels". In: *IEEE Transactions on Information Forensics and Security* 13.11 (2018), pp. 2884–2896.
- [64] Nicolas Rahmouni et al. "Distinguishing computer graphics from natural images using convolution neural networks". In: 2017 IEEE workshop on information forensics and security (WIFS). IEEE. 2017, pp. 1–6.
- [65] Huy H Nguyen et al. "Modular convolutional neural network for discriminating between computer-generated images and photographic images". In: *Proceedings of*

- the 13th international conference on availability, reliability and security. 2018, pp. 1–10.
- [66] Sanghyun Woo et al. "Cbam: Convolutional block attention module". In: *Proceedings of the European conference on computer vision (ECCV)*. 2018, pp. 3–19.
- [67] Jiaming Li et al. "Frequency-aware discriminative feature learning supervised by single-center loss for face forgery detection". In: Proceedings of the IEEE/CVF conference on computer vision and pattern recognition. 2021, pp. 6458–6467.
- [68] Jie Hu, Li Shen, and Gang Sun. "Squeeze-and-excitation networks". In: *Proceedings of the IEEE conference on computer vision and pattern recognition*. 2018, pp. 7132–7141.
- [69] iperov. *DeepFaceLab*. https://github.com/iperov/ DeepFaceLab. 2020.
- [70] Dfaker. DepFA. https://github.com/dfaker/df. 2020.
- [71] Ivan Perov et al. "DeepFaceLab: Integrated, flexible and extensible face-swapping framework". In: *arXiv* preprint arXiv:2005.05535 (2020).
- [72] Shifeng Zhang et al. "S3fd: Single shot scale-invariant face detector". In: *Proceedings of the IEEE international conference on computer vision*. 2017, pp. 192–201.
- [73] Adrian Bulat and Georgios Tzimiropoulos. "How far are we from solving the 2d & 3d face alignment problem? (and a dataset of 230,000 3d facial landmarks)". In: *Proceedings of the IEEE international conference on computer vision*. 2017, pp. 1021–1030.
- [74] Tadas Baltrusaitis et al. "Openface 2.0: Facial behavior analysis toolkit". In: 2018 13th IEEE international conference on automatic face & gesture recognition (FG 2018). IEEE. 2018, pp. 59–66.
- [75] Ricard Durall et al. "Unmasking deepfakes with simple features". In: *arXiv preprint arXiv:1911.00686* (2019).
- [76] Debin Meng et al. "Frame attention networks for facial expression recognition in videos". In: 2019 IEEE international conference on image processing (ICIP). IEEE. 2019, pp. 3866–3870.
- [77] Kaiming He et al. "Deep residual learning for image recognition". In: *Proceedings of the IEEE conference on computer vision and pattern recognition*. 2016, pp. 770–778
- [78] shanface33. *Deepfake Model Attribution Issue* 2. https://github.com/shanface33/Deepfake_Model_Attribution/issues/2. Accessed: May 11, 2023. 2023.
- [79] Andrew G Howard et al. "Mobilenets: Efficient convolutional neural networks for mobile vision applications". In: *arXiv preprint arXiv:1704.04861* (2017).
- [80] Mark Sandler et al. "Mobilenetv2: Inverted residuals and linear bottlenecks". In: *Proceedings of the IEEE conference on computer vision and pattern recognition*. 2018, pp. 4510–4520.
- [81] Mingxing Tan and Quoc Le. "Efficientnet: Rethinking model scaling for convolutional neural networks". In: *International conference on machine learning*. PMLR. 2019, pp. 6105–6114.

- [82] François Chollet. "Xception: Deep learning with depthwise separable convolutions". In: *Proceedings of the IEEE conference on computer vision and pattern recognition*. 2017, pp. 1251–1258.
- [83] Christian Szegedy et al. "Going deeper with convolutions". In: *Proceedings of the IEEE conference on computer vision and pattern recognition*. 2015, pp. 1–9.



Wasim Ahmad received his bachelor's degree in computer science from Abdul Wali Khan University Mardan, Pakistan, in 2013. He then completed his master's degree in System and Software Engineering from National Research University HSE, Moscow, Russia, in 2018. He is currently pursuing PhD under the TIGP at the Institute of Information Science, Academia Sinica, in collaboration with National Chengchi University, Taipei, Taiwan. His research interests includes Multimedia Forgery Detection and Deep Learning.



Yuan-Hao Chang (Fellow, IEEE) received his Ph.D. in Computer Science from the Department of Computer Science and Information Engineering at National Taiwan University, Taipei, Taiwan. He is currently a Research Fellow at the Institute of Information Science, Academia Sinica, Taipei, Taiwan. His research interests include memory/storage systems, operating systems, embedded systems, and real-time systems. He is a Fellow of IEEE.



Yan-Tsung Peng (Member, IEEE) received the Ph.D. degree in electrical and computer engineering from the University of California, San Diego, in 2017. In 2019, he joined the National Chengchi University, where he is currently an Assistant Professor in the Department of Computer Science. Before that, he was a Senior Engineer with Qualcomm Technologies, Inc., San Diego, CA, USA. His research interests include image processing, video compression, and machine-learning applications.



Gaddisa Olani Ganfure is currently an Assistant Professor of Computer Science at Dire Dawa University, Ethiopia. He received his bachelor's and master's degrees in computer science from Wollega University and Addis Ababa University, respectively, and his Ph.D. in Social Network Analysis and Human-Centered Computing from National Tsing Hua University in collaboration with Academia Sinica, Taiwan. His research interests include cybersecurity, artificial intelligence, and natural language processing. He has received three national patents

and published numerous papers in top-tier computer science journals.



Sarwar Khan received the BSC degree in Telecommunication Engineering from University of Engineering and Technology Peshawar, Pakistan in 2011 and ME degree in Information and Communication Technology from Kasetsart University, Thailand., in 2017. He is currently pursuing a Ph.D degree in social networks and human-centered computing with CITI, Academia Sinica. His research interests include deep learning, computer vision, and multimedia.



Sahibzada Adil Shahzad received a B.S. degree in Software Engineering from the University of Science and Technology Bannu, Pakistan, in 2016, and an M.S. degree in computer science from the Beijing Institute of Technology, China in 2019. He is currently pursuing a Ph.D. degree with the Taiwan International Graduate Program in Social Networks and Human-Centered Computing, Institute of Information Science, Academia Sinica, Taipei, Taiwan, and the Department of Computer Science, Faculty of Science, National Chengchi University, Taipei,

Taiwan. His research interests include machine learning, multimedia forensics, and image, video, and audio processing.